Trends in Biomaterials and Artificial Organs
www.biomaterials.org.in/tibao
ISSN 0971-1198
https://doi.org/10.5281/zenodo.17233574

Original Article

Barbaloin-Chitosan-Hydroxyapatite Composite: A Novel Approach of Bone Tissue Engineering Application for Dental Implant Material Development

Mohammed Yashir[1#], Ashwathi Vijayalekha[1#], Saranya Srinivasan[1], Suresh Kumar Anandasadagopan[2], Ashok Kumar Pandurangan[1*]

[1]*School of Life Sciences, B.S. Abdur Rahman Crescent Institute of Science and Technology, GST road, Vandalur, Chennai 600048, Tamil Nadu, India*
[2]*Biochemistry & Biotechnology Laboratory, CSIR-Central Leather Research Institute, Adyar, Chennai, India*

Received: *21 February 2025*
Accepted: *22 April 2025*
Published online: *30 September 2025*

Keywords: *barbaloin, chitosan, hydroxyapatite, scaffold, dental implant*

Dental implants are a common solution for tooth loss, however, traditional procedures involve multiple phases, extended recovery times, and high costs. To overcome these challenges, this study explores a novel chitosan (CH)-based implant material incorporating barbaloin (BR) and hydroxyapatite (HAP), fabricated using the sol-gel method. Barbaloin, a bioactive compound derived from Aloe vera, possesses antioxidant, anti-inflammatory, and anticancer properties, making it a promising additive for enhancing scaffold bioactivity. This study investigates the effects of varying barbaloin concentrations on the physicochemical and biological properties of the BR/CH/HAP composite scaffold. Structural and chemical characterization was performed using Scanning Electron Microscopy (SEM), Fourier-transform Infrared Spectroscopy (FTIR), and Thermogravimetric Analysis (TGA). Biochemical assessments, including swelling behavior, porosity, and scavenging potential, were conducted to evaluate its suitability for bone regeneration. Additionally, in vitro biocompatibility was assessed using human osteoblast-like MG-63 cells, while acute toxicity of BR was evaluated in zebrafish embryos. The findings highlight the BR/CH/HAP scaffold as a promising biomaterial that mimics the structure and function of native bone tissue, offering an effective and biocompatible alternative for dental implants. This study underscores its potential as a next-generation implant material, paving the way for improved and cost-effective dental treatments.

Introduction

Dental implants serve as a crucial solution for restoring lost teeth, particularly when no other alternative exists for replacing missing teeth at edentulous sites. Advances in modern dental implantology have introduced various materials and surgical techniques to improve implant success rates [1]. Among these, metallic implants are widely used due to their excellent mechanical strength, corrosion resistance, and biocompatibility. However, a major limitation of metallic implants is their poor osseointegration, which necessitates an extended healing period of three to six months for successful implant integration. In orthodontics, micro-implants are often employed for controlled tooth movement and anchorage in fixed appliance therapy [2].

To enhance implant performance and osseointegration, researchers have explored composite coatings for metallic implants [3]. Chitosan (CH), a natural biopolymer, has gained significant attention for its biocompatibility, biodegradability, and antimicrobial properties. Its intrinsic binding abilities facilitate strong adhesion between coatings and substrates. Additionally, chitosan can be processed into various forms such as films, gels, sponges, and microspheres, making it highly versatile for biomedical applications [4]. Due to its low cost and natural origin, chitosan has been extensively studied for use in wound healing, drug delivery, infection control, and bone regeneration [5].

Another essential component in bone tissue engineering is hydroxyapatite (HAP), a calcium phosphate material that closely resembles the mineral composition of natural bone and teeth. HAP is widely recognized for its osteoconductivity, bioactivity, and biocompatibility, making it a preferred material for dental implants, bone grafts, and orthopedic applications [6]. HAP has

* *Coresponding author*
E-mail address: ashokkumar.sls@crescent.education *(Dr. Ashok Kumar Pandurangan, Associate Professor, School of Life Sciences, B.S. Abdur Rahman Crescent Institute of Science and Technology, GST road, Vandalur, Chennai 600048, India)*

also demonstrated antibacterial properties, making it beneficial for preventing post-implant infections [7]. In this study, chitosan-hydroxyapatite (CH/HAP) composite scaffolds were fabricated using a freeze-drying method, without the need for cross-linking agents, to evaluate their structural and functional properties .

To further enhance the biological activity of CH/HAP scaffolds, barbaloin, a secondary phytoconstituent from Aloe species, was incorporated. Barbaloin (10-beta-D-glucopyranosyl-1,8-dihydroxy-3-hydroxymethyl-9(10H)-anthracenone) is primarily found in Aloe leaves, with its highest concentration in younger leaves. Barbaloin is known for its antimicrobial, anti-inflammatory, antioxidant, anticancer, and wound-healing properties, making it a valuable bioactive compound in regenerative medicine. Due to its potent pharmacological properties, barbaloin has been used in medicinal formulations, including creams, gels, and dietary supplements, particularly for skin regeneration and wound healing [8]. However, its application in dental implants and bone tissue engineering remains largely unexplored.

Given the significance of scaffold materials in tissue regeneration, this study aims to develop and characterize a novel barbaloin-chitosan-hydroxyapatite (BR/CH/HAP) composite scaffold for potential applications in dental implants. Since successful implant integration depends on soft tissue adhesion and bone regeneration, the study explores the biological and mechanical properties of the BR/CH/HAP scaffold. Although scaffold materials have been extensively studied for bone and skin wound healing, their adaptations for oral applications remain limited.

Materials and Methods

Chitosan, medium molecular weight deacetylated chitin, poly(D-glucosamine) (product code: 448877) 75-85% deacetylated with quality level of 200 in powder form and viscosity is 200-800 cP, 1wt. % in 1% acetic acid was procured from Sigma Aldrich. Hydroxyapatite was synthesized by wet chemical precipitation method and characterized, Barbaloin was procured from Yucca Enterprises, Mumbai, India. Zebrafish embryos from Tharun fish farm, Manimangalam, Chennai, India. All other chemicals used were of analytical grade.

Zebrafish maintenance and developmental toxicity

The zebra fish larvae were kept at 28°C on a light: dark cycle of 14:10 hours. After natural spawning, embryos were harvested and incubated at 28°C. The model group's zebrafish larvae were split into seven groups at random and transferred to 24-well plates. To get varying concentrations, we diluted the stock solution with E3 media after dissolving the barbaloin in ethanol solvent ranging from 3.125, 6.25, 12.5, 25, 50 and 100 µg/ml concentartion 1ml of E3 media. Zebrafish embryo development was monitored for 96 hours post-fertilization (hpf). This included survival and hatching rates and assessing morphological anomalies. The non-viable eggs were removed during the assessment [9].

Fabrication of BR/CH/HAP composite scaffold

The biomaterial composite was designed by incorporating chitosan, hydroxyapatite, and barbaloin. The concentrations of chitosan (2% w/v) and hydroxyapatite (1% w/v) are kept constant. Varying concentrations of barbaloin were established to detest the potential nature of the scaffold for the bone regeneration. In table 1, the different concentrations of barbaloin are 5%, 15% and 20% were denoted as 5BR/CH/HAP, 15BR/CH/HAP, and 20BR/CH/HAP which were acquired from the results of developmental toxicity tests and biochemical assays. The mixture of bio-composites was

Table 1: Treatment groups of fabricate scaffold based on the varying concentrations of barbaloin

	Treatment groups	Barbaloin (w/v)	Chitosan (w/v)	HAP (w/v)	Scaffold
1	CH/HAP (Chitosan/ Hydroxyapatite)	-	2%	1%	
2	5BR/CH/HAP (5% Barbaloin/ Chitosan/ Hydroxyapatite)	5%	2%	1%	
3	15BR/CH/HAP (15% Barbaloin/ Chitosan/ Hydroxyapatite)	15%	2%	1%	
4	20BR/CH/HAP (20% Barbaloin /Chitosan/ Hydroxyapatite)	20%	2%	1%	

lyophilized using a freeze-dryer at -70C and 0.001 mbar for 3 days. The obtained samples of porous scaffolds were vacuum-sealed for storage.

Physicochemical characterization of fabrication scaffold

To evaluate possible interactions between the CH/HAP and BR/CH/HAP scaffolds, FTIR analysis was carried out using a Perkin Elmer Spectrum100 equipment in the horizontal attenuated total reflectance mode in the wavenumber range of 400 to 4000 cm^{-1}. The thermal property of the BR/CH/HAP scaffolds was examined using thermogravimetry analysis (TGA). A Metter Toledo TGA Stare System was used to perform the thermogravimetric analysis. It had a scan range of 25 to 600°C, a heating rate of 20°C per minute, and a flux of 60 mL/min for nitrogen as a protective gas and air as a reactive gas. The samples morphology and micro-structure were examined using a scanning electron microscope (SEM). The seeded membranes and other manufactured samples were morphologically characterized using an energy-dispersive spectrometer (EDX) EDAX Apollo connected to a scanning electron microscopy (SEM) FEI Inspect F50 system by Sophisticated Test and Instrumentation Centre Kochi, Kerala.

Biochemical characterization of fabrication scaffold

Antioxidant activity of barbaloin by DPPH assay

The Antioxidant activity and free radical scavenging activity of barbaloin scaffold was determined via 1, 1-Diphenyl-2-picrylhydrazyl (DPPH) assay. 100µl of 0.1mM acetic DPPH prepared in ethanol was mixed with 100µl of barbaloin ranging from 100µg to 1.525µg/ml on the 96 well plate. The mixture was mixed well and kept in the dark for incubation for 30 minutes. The same procedure was performed for other three positive controls known antioxidants such as gallic acid [10]. The absorbance was measured in multimode reader at 517 nm. The scavenging activity of scaffold was calculated as follows, where $A_{cont.}$ and A_{test} are absorption of control and test respectivly.

DPPH Scavenging activity (%) = $(A_{cont.} - A_{test})/(A_{cont.}) \times 100$

Swelling testing

To determine the scaffolds' swelling ratio, lyophilized scaffolds were weighed (Wd) and submerged in phosphate buffer saline solution (PBS) at 370°C for 30, 60, and 120 minutes. After absorbing by surplus solution that remained on the surface of the swollen scaffolds using filter paper, the scaffolds were weighed (Ws) [11]. The following equation was used to determine the scaffold's swelling ratio.

Table 2: morphological parameters of zebrafish larvae on Barbaloin extract showed no changes compared to the control

Parameters	Concetration of barbaloin (day 4)						
	Control	3.125(µg/ml)	6.25(µg/ml)	12.5(µg/ml)	25(µg/ml)	50(µg/ml)	100(µg/ml)
Growth	NOR	NOR	NOR	NOR	NOR	NOR	NOR
Total length(mm)	322.89	341.12	344.50	341.12	356.02	344.58	344.52
Tail	NOR	NOR	NOR	NOR	NOR	NOR	NOR
Body	NOR	NOR	NOR	NOR	NOR	NOR	NOR
Facial edema	NF	NF	NF	NF	NF	NF	NF
Pigmentation	NF	NF	NF	NF	NF	NF	NF
Paricardial sac	NOR	NOR	NOR	NOR	NOR	NOR	NOR

*NOR – Normal *NF – Not found

Swelling ratio (%) = *(Ws-Wd)/ Wd x 100*

Porosity measurement

The Archimedes method was used to measure the porosity of BR/CH/HAP scaffolds. W1 was the mass of the flask containing anhydrous ethanol (up to the tick point), and Ws was the mass of the dry scaffold. The anhydrous ethanol that spilled the tick mark was sucked out and disposed of when the scaffold was completely saturated with it before being placed into the flask and weighed (W2) [12]. After the scaffold was removed, the flask's mass was marked as W3. Using, this the porosity of the scaffolds was found.

Porosity (%) = *(W3 - W2 -Ws) / (W1-W3) x 100*

In vitro biocompatibility assessment

The biocompatibility of implants was assessed using an MTT (3-(4,5-dimethylthiazol-2-yl)-2,5-diphenyltetrazolium bromide) assay. The implants were exposed to UV light for 20 minutes to ensure sterility. Conditioned media was prepared using DMEM with 10% FBS and 1% antibiotics, and the implants were incubated for 24 hours. MG-63 ($4x10^3$ per well) cells were seeded into 96-well plates and treated with the conditioned media for 24, 48, and 72 hours. Wells containing only media served as control. After treatment, MTT was added to each well and incubated for 4 hours at 37°C. The formazan crystals were then dissolved with 10% DMSO, and the optical density was measured at 570 nm using a PerkinElmer Multimode Plate Reader [13].

Results and Discussion

Acute toxicity test in Zebrafish embryos

The results from figure 1A indicate a dose-dependent effect of barbaloin on hatching rate. The control group, devoid of barbaloin, exhibited the highest hatching percentage (~100%), demonstrating normal embryonic development. At low concentrations (3.125–12.5 µg/ml), the hatching rate remained relatively unchanged compared to the control, suggesting minimal toxicity. However, at 25 µg/ml, a moderate reduction in hatching rate was observed, indicating the onset of embryotoxic effects. At higher concentrations (50 and 100 µg/ml), a significant decline in hatching rate was evident, suggesting that elevated barbaloin exposure disrupts normal embryonic development, likely through oxidative stress, impaired enzymatic function, or developmental abnormalities. These findings highlight the concentration-dependent toxicity of barbaloin, where higher doses negatively impact zebrafish embryogenesis [14].

Figure 1B represents the survival rate (%) of zebrafish larvae exposed to different concentrations of barbaloin (µg/ml) over four days post-fertilization (dpf). In, Day 1 and Day 2, the survival rates remained above 90% across all concentrations, suggesting minimal toxicity during the early stages of development. Further, in day 3, A moderate decline in survival rate is observed at higher concentrations (≥ 25 µg/ml), indicating the onset of toxic effects. The findings demonstrate that barbaloin exerts concentration-

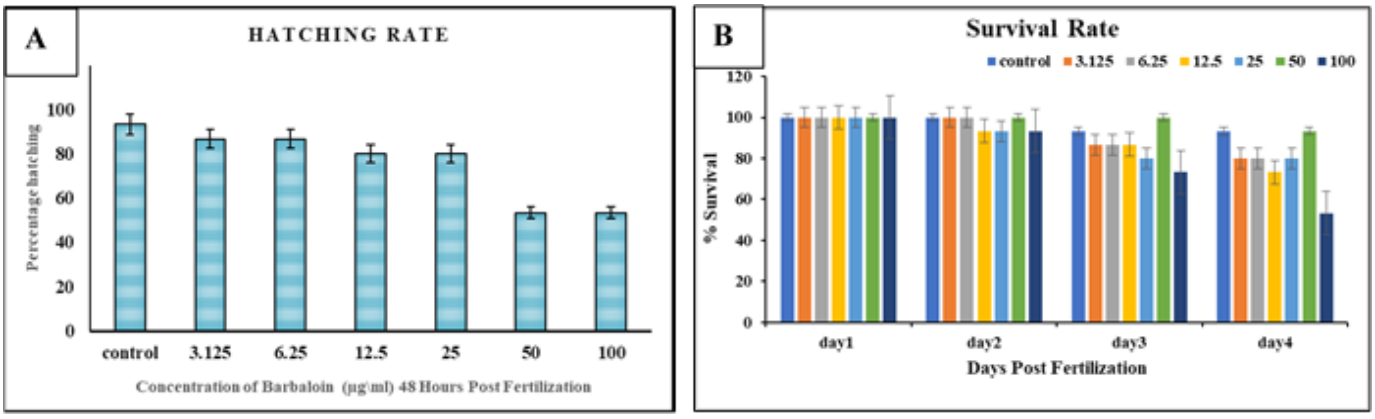

Figure 1: Zebrafish embryo Toxicity; (A) hatching rate of barbaloin at different concentrations at 48- hours post fertilization. (B) Effect of Barbaloin Concentration on Zebrafish Larval Survival Rate across Days Post-Fertilization demonstrated higher dose of Barbaloin affected its survival

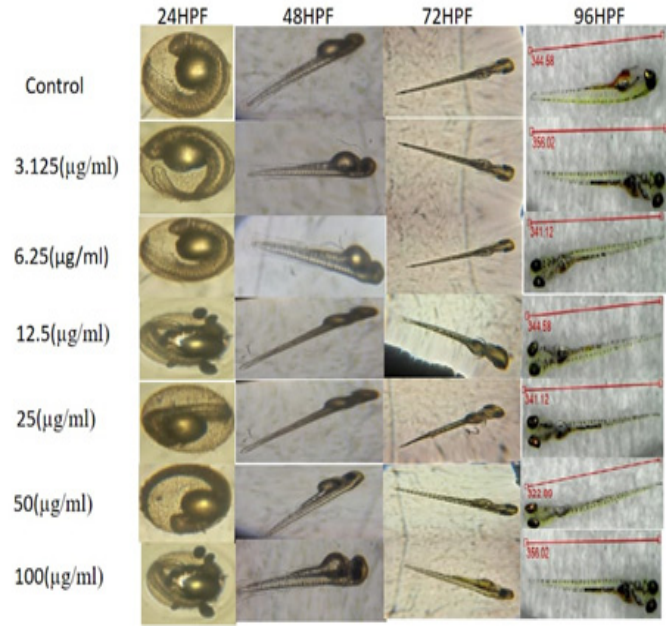

Figure 2: Morphological analysis of Barbaloin-treated zebrafish larvae till 4 days post fertilization (DPF) µg/ml

dependent toxicity on zebrafish larvae, with higher concentrations (≥ 25 µg/ml) leading to a decline in survival over time. Zebrafish embryos in specific categories were found to exhibit common morphological changes, including length of the body, tail length, coloration, pericardial sac, curved body, and curved tail as shown in table 2. Barbaloin didn't show morphological abnormalities, such as bent bodies, and tail, at any concentration; however, after 96 hours of photoperiod, changes were observed at 100µg/ml as seen in figure 2.

Biochemical characterization

Barbaloin shows more antioxidant activity compared to the all control as seen in figure 3A. Barbaloin's antioxidant activity was evaluated using the DPPH radical scavenging activity. The results showed that samples are not significantly impacted by their concentration. The antioxidant activity of the barbaloin is higher at concentrations than that of the control, gallic acid [15].

The shape, mechanical stability, and substance metabolism efficiency of the scaffolds can all be impacted by their swelling characteristics, making it a crucial component of the scaffolds. Figure 3B shows the swelling ratio of several scaffolds was investigated by immersing them in PBS for 15, 30, 60 and 120 min, respectively, to analyze their swelling behavior. Since all of the scaffolds are microporous and hydrophillic, they all exhibit good swelling properties overall [16]. All of the BR/CH/HAP scaffolds exhibit a lower swelling

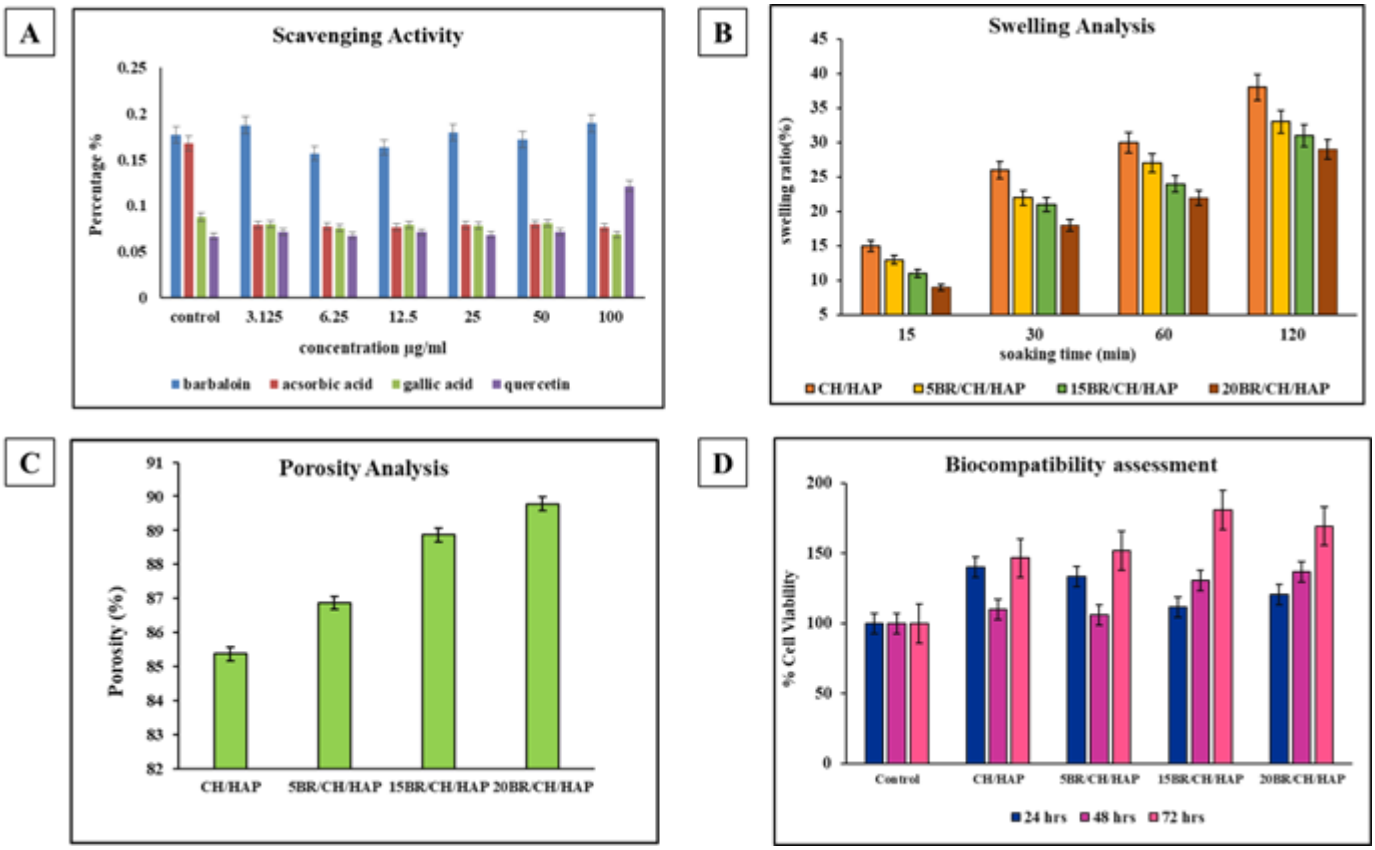

Figure 3: Biochemical Characterization of fabricated BR/CH/HAP Implant: (A) Free radical scavenging activity of Barbaloin by DPPH assay. (B) Swelling potential of fabricated implants over different time period in PBS. (C) Porosity analysis of BR/CH/HAP implants by ethanol displacement method. (D) *In vitro* Biocompatibility of Implants in human Osteoblast like MG-63 cell line over 24, 48 and 72 hours

ratio when compared to CS/HAP. The scaffold's swelling ratio decreases with increasing BR concentration. In addition all of the scaffold's swelling achieved equilibrium following a 24-hour incubation period in PBS.

A high porosity of the scaffold is generally advantageous for cell ingrowth and survival, and it plays a significant role in the regeneration of bone [17]. As seen in figure 3C, the porosity of the CH/HAP and BR/CH/HAP scaffolds was determined using the liquid replacement method. The porosity of scaffolds that are pure CH/HAP, 5BR/CH/HAP, 15BR/CH/HAP, and 20BR/CH/HAP is as follows. The porosity of the scaffold is not significantly affected by the concentration of BR. It is evident that as the BR content rises, the scaffold's porosity somewhat increases. The 20% BR/CH/HAP composite scaffold has the same level of porosity as previously mentioned.

Biocompatibility is a critical requirement for dental implant materials, as optimal osteoblast adhesion and proliferation determine successful osseointegration [18]. The results from MTT assay demonstrate that CH/HAP composites support osteoblast viability, with further improvements upon barbaloin incorporation. The dose-dependent increase in cell viability suggests that barbaloin enhances cellular activity, likely due to its bioactive properties, which may reduce oxidative stress and inflammation in the implant site (figure 3D). However, while higher concentrations of barbaloin (20BR/CH/HAP) show superior cell viability, long-term effects should be evaluated to ensure no cytotoxicity at extended exposure periods. Further *in vivo* studies will be necessary to confirm its efficacy in promoting bone regeneration within the oral cavity. Hence the study confirms that CH/HAP composites enriched with barbaloin exhibit excellent biocompatibility with osteoblast-like MG-63 cells, making them promising candidates for dental implants. The 20BR/CH/HAP scaffold demonstrates the highest osteogenic potential, suggesting that barbaloin contributes positively to bone cell proliferation. From the above results of biochemical characterization, it was evident that barbaloin played a crucial role in enhancing the implant material and hence further the effective treatment group's 5BR/CH/HAP and 20BR/CH/HAP were studied for physicochemical characterization.

Physicochemical characterization of fabrication scaffold

Figure 4 shows the FT-IR spectra of different samples CH/HAP, 5BR/CH/HAP, 20BR/CH/HAP scaffolds show broad spectrum at 3258 cm^{-1}, 3224 cm^{-1}, and 3215 cm^{-1}, which may be due to characteristic OH stretching vibration of the carboxylic acid and alcohol groups in CH/HAP, 5BR/CH/HAP, 20BR/CH/HAP respectively as shown in table 3. Characteristic peaks observed in 1030 cm^{-1}, 1035 cm^{-1}, and 1035 cm-1 were attributed to the C-N stretching or C-F stretching vibration of amine, florocompound, and sulfoxide groups as shown in table 3. The FTIR spectrum showed three spectroscopic curves were fundamentally identical [19]. The distinctive peaks of the CH/ HAP progressively become weaker as the quantity of BR increases [15,20].

Figure 5 shows the TGA on different temperature groups of CH/HAP, 5BR/CH/HAP, 20BR/CH/HAP composite scaffolds. Before being heated to 700°C at a rate of 20°C per minute with airflow, all samples were pre-treated at 100°C until a consistent weight was reached. In the temperature range under investigation, hydroxyapatite did not lose weight. As expected, the two degradation profiles - one between 250 and 350°C and the other between 450 and 580°C - showed that the scaffold's CH/HAP component had entirely oxidized [21]. It was demonstrated that the presence of barbaloin caused the first degradation profile to move to higher temperatures (between 250 and 350°C), suggesting that the CH/HAP matrix was more thermally stable in the presence

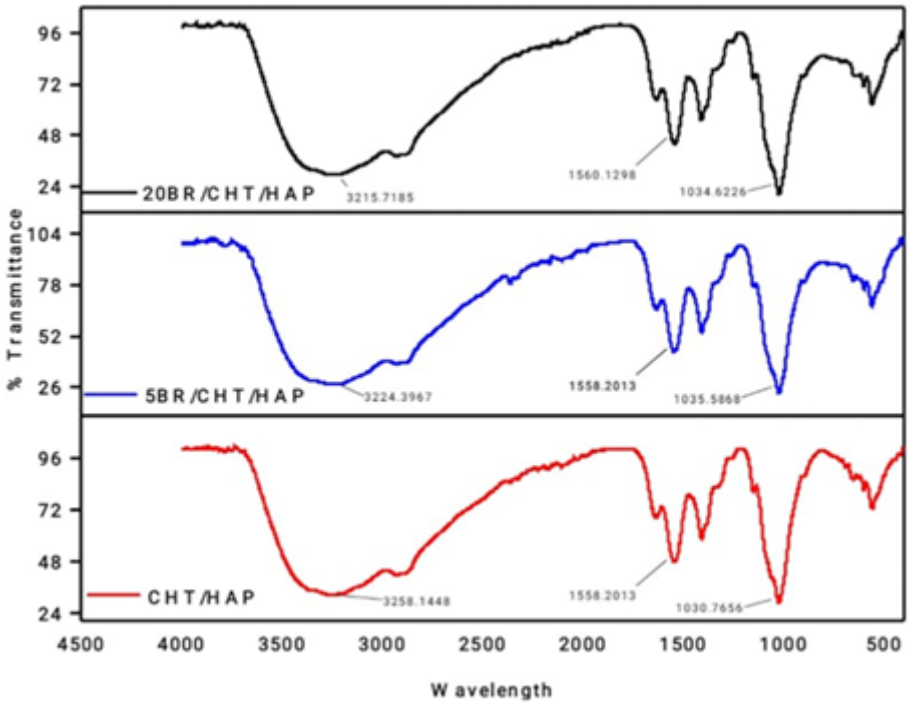

Figure 4: Fourier Transform Infrared Spectroscopy (FTIR) analysis of BR/CHT/HAP scaffold at different treatment groups

Table 3: FT-IR analysis of CH/HAP scaffolds, 5BR/CH/HAP scaffolds, and 20BR/CH/HAP scaffolds

Peak	Group	Class	Peak details
3258	O-H stretching	Alcohol, Carboxylic acid	Strong, broad
1030	C-N stretching	Amine	Medium
3224	O-H stretching	Alcohol, carboxylic acid	Strong, broad
1035	C-F stretching	Floro compound	Strong
3215	O-H stretching	Alcohol, carboxylic acid	Strong, broad
1034	S=O stretching	Sulfoxide	Strong

of inorganic materials, which most likely prevented the organic matrix from thermo-oxidizing [22].

A porous structure was also observed in the SEM image of the BR/CH/HAP scaffolds, which may have resulted from the hydroxyl groups in the NaOH solution reacting corrosively. In general, the porosity and pore size of the CH/HAP matrix are not reduced by the addition of barbaloin. The primary gaps possess an average diameter of approximately 100-200 µm and a wall thickness of about 3–5 µm. This advantageous structure facilitates the transit of nutrients and cell infiltration, hence aiding in the production of new bone [23]. The surface of the CH/HAP scaffold's pore walls is extremely smooth and clean, as shown in figure 6A. Figure 6B shows a rough pore surface on the BR/CH/HAP composite scaffold. Figure 6C shows the 20BR/CH/HAP composite scaffolds gives high porous compared to other composite scaffold.

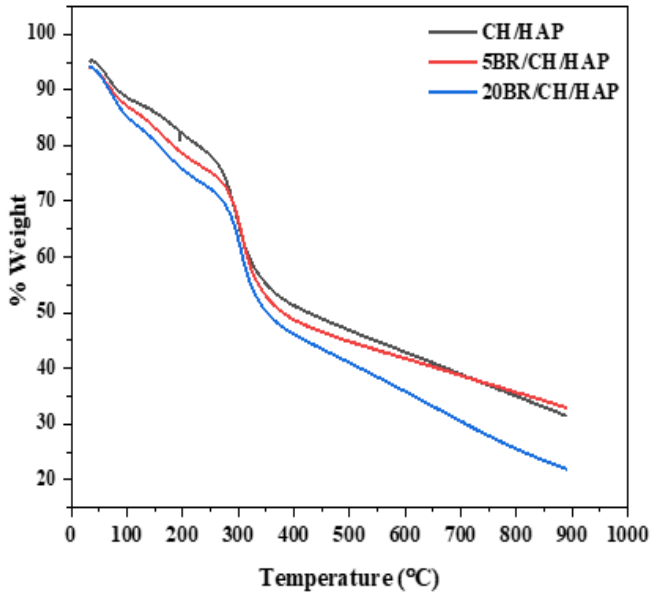

Figure 5: Thermogravimetry analysis for treatment group scaffolds BR/CH/HAP

Conclusion

This study successfully developed and characterized a novel barbaloin-chitosan-hydroxyapatite (BR/CH/HAP) composite scaffold, offering a promising alternative for dental implant applications. The integration of barbaloin, a bioactive phytochemical, into the chitosan-hydroxyapatite (CH/HAP) matrix significantly improved the scaffold's bioactivity, biocompatibility, and physicochemical properties.

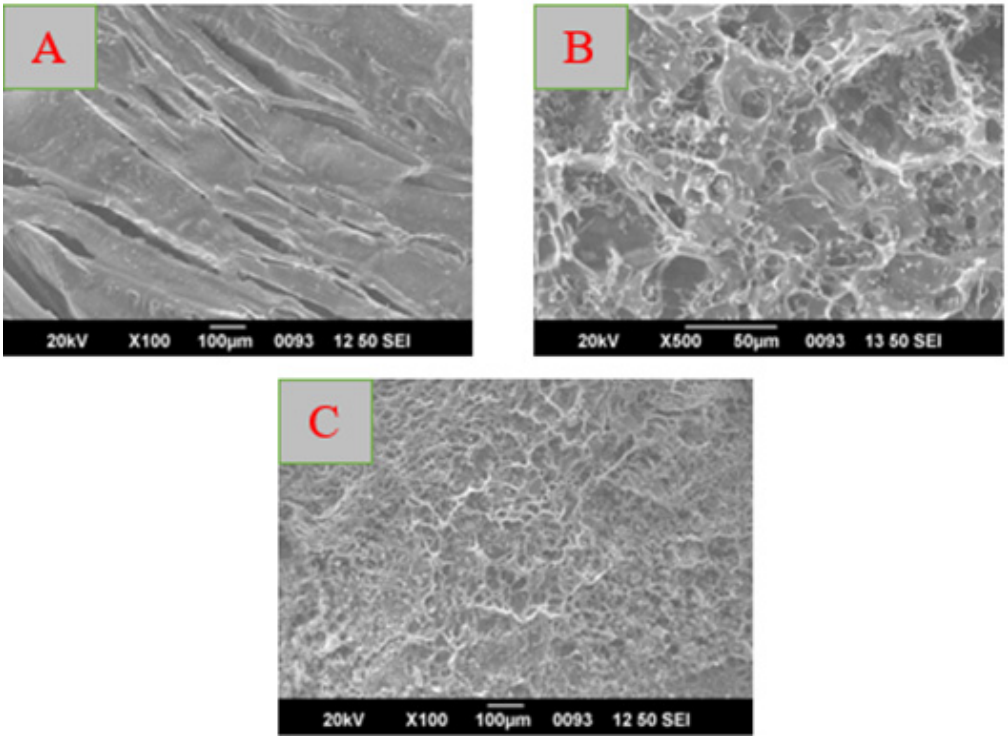

Figure 6: (A) SEM images of CH/HAP composite scaffold, (B) 5BR/CH/HAP composite scaffold, (C) 20BR/CH/HAP composite scaffold

Physicochemical analysis demonstrated that BR/CH/HAP scaffolds maintained a highly porous structure, essential for osteoblast infiltration, nutrient exchange, and vascularization, all of which are critical for successful osseointegration. Fourier-transform infrared spectroscopy confirmed the presence of functional groups responsible for enhanced cell adhesion and bioactivity, while thermogravimetric analysis indicated improved thermal stability. Scanning electron microscopy revealed a well-defined porous morphology with an interconnected network, facilitating cellular interactions and bone tissue integration.

The biochemical characterization further highlighted the scaffold's superior antioxidant activity, which may contribute to reducing oxidative stress in the implant microenvironment, thereby improving osteogenic potential and wound healing. Swelling and porosity assessments indicated that the BR/CH/HAP scaffold maintains an optimal balance of hydration and structural integrity, crucial for tissue regeneration.

Biocompatibility assessments using MG-63 human osteoblast-like cells confirmed that barbaloin incorporation enhanced cell viability, demonstrating its non-cytotoxic nature. Acute toxicity assessments in zebrafish embryos indicated a concentration-dependent effect, with lower doses exhibiting minimal toxicity. The findings indicate that the barbaloin-enriched CH/HAP scaffold is a promising biomaterial for next-generation dental implants, offering a bioactive and cost-effective alternative for clinical applications. Future studies should focus on long-term *in vivo* assessments to validate its efficacy in dental tissue regeneration.

References

1. T.M. Hamdy, Dental biomaterial scaffolds in tooth tissue engineering: a review, *Curr. Oral Heal. Reports*, 10, 14–21 (2023).
2. F. Zhao, Z. Yang, L. Liu, D. Chen, L. Shao, and X. Chen, Design and evaluation of a novel sub-scaffold dental implant system based on the osteoinduction of micro-nano bioactive glass, *Biomater. Transl.*, 1, 82 (2020).
3. H. Naujokat, Y. Açil, S. Harder, M. Lipp, F. Böhrnsen, and J. Wiltfang, Osseointegration of dental implants in ectopic engineered bone in three different scaffold materials, *Int. J. Oral Maxillofac. Surg.*, 49, 135–142 (2020).
4. S. Husain *et al.*, Chitosan biomaterials for current and potential dental applications," *Materials (Basel).*, 10, 602 (2017).
5. L. Hallmann and M.-D. Gerngroß, Chitosan and its application in dental implantology, *J. Stomatol. oral Maxillofac. Surg.*, 123, e701–e707 (2022).
6. J.L. Ong and D.C.N. Chan, Hydroxyapatite and their use as coatings in dental implants: a review, *Crit. Rev. Biomed. Eng.*, 28, 667-707 (2000).
7. F. Sharifianjazi, A.H. Pakseresht, M.S. Asl, A. Esmaeilkhanian, H. W. Jang, and M. Shokouhimehr, Hydroxyapatite consolidated by zirconia: applications for dental implant, *J. Compos. Compd.*, 2, 26–34 (2020).
8. N. Wang, G. Gan, J. Yang, and L. Wang, Barbaloin promotes osteogenic differentiation of human bone marrow mesenchymal stem cells: involvement of Wnt/â-catenin signaling pathway, *Curr. Med. Chem.*, 29, 6100–6111 (2022).
9. B. Santhosh Kumar, R. Deepachitra, P. Prabu, and T. P. Sastry, Osteoinductive potential of biocomposite cylinders impregnated with Glycyrrhiza glabra for bone tissue engineering, *Ceram. Int.*, 41, 7704–7712 (2015). *doi: 10.1016/j.ceramint.2015.02.101*.
10. A. Yagi, A. Kabash, N. Okamura, H. Haraguchi, S. M. Moustafa, and T. I. Khalifa, "Antioxidant, free radical scavenging and anti-inflammatory effects of aloesin derivatives in Aloe vera," *Planta Med.*, 68, 957–960 (2002).
11. S. Pathmanapan, P. Periyathambi, and S.K. Anandasadagopan, Fibrin hydrogel incorporated with graphene oxide functionalized nanocomposite scaffolds for bone repair — In vitro and in vivo study, *Nanomedicine Nanotechnology, Biol. Med.*, 29, 102251 (2020). *doi: 10.1016/j.nano.2020.102251*.
12. P.S. Kaparekar, S. Pathmanapan, and S.K. Anandasadagopan, Polymeric scaffold of Gallic acid loaded chitosan nanoparticles infused with collagen-fibrin for wound dressing application, *Int. J. Biol. Macromol.*, 165, 930–947 (2020). *doi: 10.1016/j.ijbiomac.2020.09.212*.
13. S. Pathmanapan, A. Muthuramalingam, A.K. Pandurangan, N. Ayyadurai, and S.K. Anandasadagopan, Hyaluronic Acid-based Cell-free Composite Scaffold Promotes Osteochondral Repair In Vitro by Upregulating Osteogenic- and Chondrogenic-Specific Gene Expressions," *Advanced Engineering Materials*, 26, 10 (2024). *doi: 10.1002/adem.202300815*.
14. S. Vimalraj, S. Saravanan, and R. Subramanian, Rutin-Zn(II) complex promotes bone formation - A concise assessment in human dental pulp stem cells and zebrafish, *Chem. Biol. Interact.*, 349, 109674 (2021). *doi: 10.1016/j.cbi.2021.109674*.
15. S. Borse, S. Nangare, P. Bafna, P. Jain, and L. Zawar, Barbaloin loaded chitosan-gum kondagogu polyelectrolyte complex based biocomposites film for enhanced antibacterial, antioxidant and wound healing activity, *Surfaces and Interfaces*, 56, 105506 (2025).
16. H.-D. Wu, D.-Y. Ji, W.-J. Chang, J.-C. Yang, and S.-Y. Lee, Chitosan-based polyelectrolyte complex scaffolds with antibacterial properties for treating dental bone defects, *Mater. Sci. Eng. C*, 32, 207–214 (2012).
17. S.C.C.C. Miranda, G.A.B. Silva, R.C.R. Hell, M.D. Martins, J.B. Alves, and A.M. Goes, Three-dimensional culture of rat BMMSCs in a porous chitosan-gelatin scaffold: A promising association for bone tissue engineering in oral reconstruction, *Arch. Oral Biol.*, 56, 1–15 (2011).
18. A.M. Preethi and J.R. Bellare, Concomitant effect of quercetin-and magnesium-doped calcium silicate on the osteogenic and antibacterial activity of scaffolds for bone regeneration, *Antibiotics*, 10, 1170 (2021).
19. C.-H. Lin, Y.-S. Chen, W.-L. Huang, T.-C. Hung, and T.-C. Wen, Hydroxyapatite formation with the interface of chitin and chitosan, *J. Taiwan Inst. Chem. Eng.*, 118, 294–300 (2021).
20. B.J. Gutiérrez Rafael, O. Zaca Moran, R.J. Delgado Macuil, H. Martínez Gutiérrez, M. García Juárez, and V. Lopez Gayou, Study of the Incorporation of Gel and Aloe vera Peel Extract in a Polymer Matrix Based on Polyvinylpyrrolidone, *Polymers (Basel).*, 16, 1998 (2024).
21. N. Akartasse *et al.*, Chitosan-hydroxyapatite bio-based composite in film form: synthesis and application in wastewater, *Polymers (Basel).*, 14, 4265 (2022).
22. R. Durga, N. Jimenez, S. Ramanathan, P. Suraneni, and W.J. Pestle, Use of thermogravimetric analysis to estimate collagen and hydroxyapatite contents in archaeological bone, *J. Archaeol. Sci.*, 145, 105644 (2022).
23. H. Zhao, J. Liao, F. Wu, and J. Shi, Mechanical strength improvement of chitosan/hydroxyapatite scaffolds by coating and cross-linking, *J. Mech. Behav. Biomed. Mater.*, 114, 104169 (2021).